https://pubs.acs.org/doi/abs/10.1021/ac504545w

Development of a Particle-Trap Preconcentration-Soft Ionization Mass Spectrometric Technique for the Quantification of Mercury Halides in Air

Daniel A. Deeds, Avik Ghoshdastidar, Farhad Raofie, Élise-AndreéGueŕette, Alain Tessier, and Parisa A. Ariya

Abstract

Measurement of oxidized mercury, Hg(II), in the atmosphere poses a significant analytical challenge as Hg(II) is present at ultra-trace concentrations (picograms per cubic meter air). Current technologies are sufficiently sensitive to measure the total Hg present as Hg(II) but cannot determine the chemical speciation of Hg(II). We detail here the development of a soft ionization mass spectrometric technique coupled with preconcentration onto nano- or microparticle-based traps prior to analysis for the measurement of mercury halides in air. The current methodology has comparable detection limits (4−11 pg m^{-3}) to previously developed techniques for the measurement of total inorganic mercury in air while allowing for the identification of HgX_2 in collected samples. Both mercury chloride and mercury bromide have been sporadically detected in Montreal urban and indoor air using atmospheric pressure chemical ionization-mass spectrometry (APCI-MS). We discuss limitations and advantages of the current technique and discuss potential avenues for future research including quantitative trace measurements of a larger range of mercury compounds.

Mercury, a toxic heavy metal that bioaccumulates up aquatic food chains,[1] is elevated above preindustrial levels in the environment due primarily to emissions associated with precious metals mining and coal-fired power plant production.[2,3] The oxidation state (0 vs II) and phase of anthropogenic mercury (gaseous vs particle-bound) largely determines its removal rate from the atmosphere,[4,5] with $Hg(0)_{(g)}$ being relatively insoluble and inert compared to $Hg(II)_{(g)}$ or particle-bound Hg.[4,5] Understanding the chemical makeup of anthropogenic mercury emissions and subsequent chemical transformations after release is a crucial step toward assessing the balance between mercury deposition to nearby soils and waterways[4−6] and transport to remote, pristine environments (e.g., the Arctic).[7]

Current atmospheric mercury measurements are mainly limited to the study of bulk mercury reservoirs: specifically, mercury is measured as gaseous elemental mercury (GEM, Hg^0), as Hg^0 derived from the chemical reduction or pyrolysis of gaseous oxidized mercury (GOM, or reactive gaseous community. Methods for the measurement of GOM are presented in Table S1, Supporting Information.[8−14]

Intercomparison of mercury speciation methods, including equivalent instrumentation, has shown large differences in measured mercury speciation,[15] attributed to incomplete mercury capture and to wall losses or heterogeneous reactions in the sampling manifold. In addition, KCl denuder-cold vapor atomic fluorescence spectroscopy (CV-AFS), a technique often used to measure GOM, may preferentially collect certain types of Hg(II)[14] and is susceptible to passivation by atmospheric oxidants and humidity at atmospherically relevant concentrations.[16,17]

Thermal decomposition to Hg^0 allows for sensitive detection of total GOM or $Hg_{(P)}$ but destroys their chemical identity. These measurements provide insight into the transfer of mercury between the atmosphere, waters, snow, and soils (e.g., refs 6, 7, 18−20) but may not necessarily inform one about rates of deposition to, reemission from, and methylation in aquatic environments.[1] The direct chemical speciation of mercury in the atmosphere would close crucial gaps in the geochemistry of mercury, providing better ability to assess the impact of mercury emissions on the environment. Gas chromatography−mass spectrometry has been used to directly identify mercuric nitrate and mercury chloride in simulated flue gases, but the concentrations involved (μg Hg m^{-3}) are significantly higher than the atmospheric GOM background.[11] Recent method development has begun to address the chemical speciation of mercury

through thermal decomposition profiles of captured Hg,[15] but profiles produced are complicated by codesorption of contaminants.

Mercury halides (HgX_2, X = Cl, Br, I) are thought to be one of the principal forms of oxidized mercury in the atmosphere.[4,5] In particular, $HgBr_2$ is implicated in atmospheric mercury depletion events observed at the poles[7] and midlatitudes.[15] As of yet, mercury halides have not been directly observed in the atmosphere; their presence in air is instead inferred from correlations of GOM with atmospheric oxidants such as BrO and Br.[15] Other potential forms of Hg(II) are HgO, $HgSO_4$, $Hg(NO_2)_2$, and $Hg(OH)_2$.[21−23]

We report here an analytical methodology for the detection of mercury halides at atmospherically relevant concentrations (10^{-12} g Hg m^{-3} air) by nano- or micro-particle trapping coupled with atmospheric pressure chemical ionization-mass spectrometry (APCI-MS). We also present initial measurements of mercury halides in urban and indoor air. The limitations and potential future applications of the technique will be discussed.

METHOD DEVELOPMENT

This section details the tests taken to address the analytical challenge posed by the trace quantities of oxidized mercury present in the atmosphere. We discuss APCI optimization through selection of a CI gas for facile HgX_2 identification (APCI Source Parameter Optimization) while minimizing side products and the selection of APCI ionization parameters to improve ion production and transmission into the MS. We then discuss development of particle-based sorbent traps (Sorbent Trap Packing) for HgX_2 collection from ambient air (HgX_2 Breakthrough and Retention). We end by detailing initial tests of the complete APCI-MS system in urban and indoor air (Air Analyses, McGill University, Montreal Quebec, Canada).

Source Modification and CI Gas Selection. Gas phase HgX_2 species were detected using an Agilent 6130 single quadrupole MS with APCI ion source installed. APCI-MS was chosen over electron ionization MS (EI-MS) as EI-MS fragments HgX_2 into Hg^+ and X^- ions (Figure S1a, Supporting Information) that are indistinguishable from those produced by elemental mercury or halogenated species in air extracts. EI-MS can produce small amounts of molecular ion for Hg(II) detection[11] but only at high concentrations applicable to extreme atmospheric conditions (e.g., power plant flue gas).

In contrast, APCI is a "soft" ionization producing mainly molecular ions with less fragmentation than EI-MS due to indirect ionization via a solvent and due to minimal wall-losses and ion thermalization at the ambient pressures of the inlet (Figure S1b, Supporting Information). The APCI inlet of the Agilent 6130 nebulizes aqueous samples for gas-phase analysis; we removed the inlet nebulizer and widened the inlet to accommodate a 6 mm gas-line or sorbent trap (Figure S2, Supporting Information). A programmable oven heats the inlet, such that wall losses of analytes are minimized or desorption of analytes can be performed.

Moving from aqueous- to gas-phase APCI analysis required the replacement of the solvent with a reagent gas. Ionization via charge transfer from nitrogen resulted in high residual energy on ionized HgX_2, causing extensive ion fragmentation (Figure S3a,b, Supporting Information). A variety of CI reagent gases were tested for retention of incoming mercury species (Table 1). In almost all tests, the CI gas was supplied by placing a 3 L dual side-arm glass flask containing 1 atm of reagent gas in-line between a UHP nitrogen tank (at 80 psig, flowing at 1 L min^{-1}) and a 6 L dual side-arm glass flask containing HgX_2 powder (∼10 g) under a nitrogen headspace. Nitrogen gas from the tank mixed sequentially with CI gas and HgX_2-rich gas in the 3 and 6 L flasks, respectively, prior to entering the APCI ion source. One-hour tests showed no signal decrease from HgX_2 standards, indicating a constant flux of mercury halide over this time period. Continuous scan-mode monitoring of masses in negative-ion mode ($175 \leq m/z \leq 550$) allowed for detection of ions formed from incoming HgX_2 as the reagent gas was diluted with the nitrogen pushing gas. Qualitative results of CI gas tests are presented in Table 1. Several aqueous phase analyses are presented as well, including one for mercuric oxide. Aqueous mercuric oxide (at pH = 7) was detected as $[Hg(OH)_2]^+$ using positive-mode APCI. Early tests on CI gases were performed using a Waters Micromass Quattro tandem quadrupole LC-MS at the Center for Biological Applications of Mass Spectrometry (CBAMS) at Concordia University. The Quattro LC-MS inlet line for aqueous analytes was replaced by 6.3 mm PTFE tubing for direct

connection to HgX_2 standards.

Tests for the CI blend of isobutane (MEGS, >99.5% purity) and sulfur hexafluoride (MEGS, >99.95% purity) replaced the 3 L flask and nitrogen tank with pressurized tanks whose outflow were controlled via flowmeters to a total flow of 1 L min^{-1} (at 10 psig). The standard used for these tests consisted of 5-mesh HgX_2 pellets or powder packed into a 6 mm ID PFA tubing with dichlorodimethylsilane (DCDMS)-coated glass wool or Teflon septa (Figure S4, Supporting Information). We transitioned from the flask standard to packed standards as they were more compact, portable, and easier to manipulate in the laboratory. Packed standards were calibrated by repeat measurement of emitted HgX_2 by KCl denuder coupled with CV/AFS. The KCl denuder was found to collect 90 ± 6% (n = 26) of incoming Hg(II) from standards based on CV/AFS analysis during sampling of standards vs during denuder heating at 500 °C (Figure S5, Supporting Information). HgX_2 packed standards emitted Hg concentrations of 50 ± 20 ng Hg L^{-1}.

Mercury halides preferentially undergo complexation with other constituents in the ion source (Table 1). Many of the ions observed can be attributed to atmospheric contaminants, such as $(H_2O)^-$ ($m/z = n \times 18$) or O^- (m/z = 16). Masses of m/z =19, 35, and 80 correspond to the halides F^-, Cl^-, and Br^-. The APCI source for the Agilent single quadrupole MS was freer of contaminants than the Waters tandem quadrupole MS: the Agilent MS produced only $[HgCl_3]^-$ with 100% N_2 (Figure S3a, Supporting Information). The presence of HgX_3^- ions suggests that fragmentation occurred, although it was mainly limited to when the reagent gas recombination energy (equivalent in magnitude to its ionization potential) was greater than the analyte's ionization energy. In this case, the residual energy left after charge transfer resulted in ion fragmentation.

Of the CI gases studied, we initially selected isobutane (IB) as it produced simple spectra consisting of an ion complex ($[M+ 26]^-$) of the analyte and an isobutane fragment (m/z = 26, speculated to be C_2H_2) and small peaks corresponding to the molecular ion and to trihalide ions (e.g., $[HgCl_3]^-$, $[HgBr_2Cl]^-$). Isobutane and UHP nitrogen were blended in proportions of 0−100% IB/N_2 using flowmeters (total flow of 1 L min^{-1} at 10 psig) connected by a PFA tee to a single HgX_2 packed standard connected directly to the APCI inlet. A blend of 10:90 IB/N_2 was selected as a compromise between high sensitivity detection of both $HgCl_2$ and $HgBr_2$ and economizing reagent gases (Figure S6, Supporting Information). We note that direct chemical identification of Hg(II) via $[M]^-$ was possible using 100% IB as a CI gas, but the relative yield of $[M]^-$ in selected ion monitoring (SIM) mode (e.g., 1.2×10^4 cts) was an order of magnitude less than the yield of $[M + 26]^-$ for the same standard with a 10:90 IB/N_2 CI gas (e.g., 2.2×10^5 cts in SIM mode).

To test for analyte loss to in-source reactions, we introduced both $HgCl_2$ and $HgBr_2$ into the APCI ion source from a 50:50 (by mass) $HgCl_2$/$HgBr_2$ standard consisting of 5-mesh HgX_2 particles in a 6 mm ID PFA tube packed between Teflon septa. The mixed standard source was placed upstream of a shredded Teflon sorbent trap (discussed below in Sorbent Trap Desorption: Timing and Temperature and Sorbent Trap Packing), blanked at 200 °C in the APCI inlet, and connected to a field pump. HgX_2 was collected onto the trap for 1 min at 1 L min^{-1} prior to desorption into the APCI source at 200 °C with a 10:90 IB/N_2 CI gas flowing through the trap at 1 L min^{-1}. $HgCl_2$ and $HgBr_2$ sequentially desorb from the trap into the APCI source (Figure S7, Supporting Information). The major ion observed during APCI-MS analysis of the mixed halide was m/z = 343, corresponding to $[HgBrCl + 26]^-$. HgBrCl was detected only after both HgX_2 compounds are present in the APCI inlet suggesting that HgBrCl was an artifact of ion reactions rather than being a desorbed analyte. Currently, HgBrCl cannot be considered a legitimate environ- mental signal if detected in air extracts.

In an attempt to limit ion reactions in the APCI inlet, we analyzed the HgCl /HgBr standard using a sulfur hexa uoride/IB blend as a CI gas. Sulfur hexafluoride (SF_6), a strong electron acceptor,[24] decomposed into $SF_5^+ + F^-$ in the APCI ion source (Figure S8, Supporting Information). Fluoride ion complexed with HgX_2 to produce m/z = 291 ($[HgCl_2F]$; 40% relative abundance), m/z = 336 ($[HgBrClF]^-$; 100% relative abundance), and m/z = 381 ($[HgBr_2F]^-$; 80% relative abundance). Although the SF_6/IB CI gas does not prevent in-source ion reactions, it provides a complementary analysis yielding alternate ions that may aid in positive identification of HgX_2 where contaminants are present at m/z of $[M + 26]^-$.

Target ion abundances in scan-mode spectra with CI by IB/N_2 and SF6/IB were comparable, with principal ion abundances on the order of $(2-3) \times 10^4$ cts. The yields of $[M + F]^-$ for blends of 0.5:99.5 to 99.5:0.5 SF_6/IB were relatively constant suggesting that HgX_2 supplies a limited ion complex formation rather than F^- production. To conserve SF_6, a 0.5% SF_6 in IB blend was used for all subsequent SF_6/IB tests.

Sorbent Trap Desorption: Timing and Temperature. Direct insertion of HgX_2 standards into the APCI inlet led to persistent blanks (e.g Figure S3b, Supporting Information) and signal degradation over time. To introduce controlled, smaller quantities of analyte, we collected HgX_2 onto homemade sorbent traps consisting of 6 mm ID glass tubing packed with copper-doped iron nanoparticles silanized with bis[3-(triethox- ysilyl) propoyl] tetrasulfide[25] electrostatically held on 5 μm glass beads or with shredded PFA tubing, held in place with glass wool and stainless-steel wire (Figure S9, Supporting Information). Standards were connected with PFA connectors upstream of a sorbent trap attached to a field pump, with flow controlled to 1 L min^{-1} by an acrylic flowmeter downstream of the trap (Figure S10, Supporting Information). After pumping, a sorbent trap was immediately connected to a gas line teed to CI gases via a blanked PFA elbow and inserted into the APCI inlet. Initial tests indicated an optimal desorption temperature of 200 °C, with CI gas flow starting at 0.2 min after insertion (Figure S11, Supporting Information). A decreased signal at 225 °C may result from thermal decomposition of HgX_2.[26] A desorption of 1.2 min was sufficient to release captured analyte into the APCI inlet. Unless stated otherwise, the following tests involve HgX_2 collection over 1 min followed by desorption into the APCI inlet as described in this section.

APCI Source Parameter Optimization. Ion production in the APCI source is controlled through manipulation of three main parameters: the current through the corona discharge pin, the voltage applied across the capillary between the APCI source and MS, and the voltage excess applied to the fragmentor, a charged section between the capillary and MS that accelerates ions for controlled fragmentation. These parameters control coronal intensity, in-source fragmentation, and ion complexation (corona current), as well as ion transmission to the MS (capillary and fragmentor voltage).

APCI analyses of $HgCl_2$ and/or $HgBr_2$ collected on polysulfide traps for 1 min at 1 L min^{-1} (Sorbent Trap Desorption: Timing and Temperature) using the IB/N_2 CI gas were taken at corona currents of 10, 20, 30, and 40 μA. For each step in corona current, triplicate measurements using capillary voltages of 500, 1500, 3000, and 4000 V were taken. For each capillary voltage, the fragmentor voltage was set to 20, 40, and 60 V above the capillary voltage. Inlet and drying gas temperatures were set to 200 °C with a drying gas flow rate of 3 L min^{-1}. HgX_2 detected in SIM mode for *m*/*z* of 294−301 ($HgCl_2$) and 382− 391 ($HgBr_2$), with the principal signal for the compounds taken as the height of m/z = 298 and 388, respectively.

$HgCl_2$ and $HgBr_2$ ion production and transmission using SF_6/IB were also tested for 1 min extracts of air passing through the mixed HgX_2 standard onto a shredded Teflon trap, at capillary voltages of 500, 750, 1500, 2500, and 4000 V (30 μA corona current) and at corona currents of 1, 5, 10, 20, 30, and 40 μA (750 V capillary voltage). Drying gas and inlet temperatures were set to 200 °C with a drying gas flow rate of 5 L min−1 , and the fragmentor excess voltage was set to 60 V. A series of tests at fragmentor voltages of 20, 40, 60, 80, 100, 120, and 140 V was also performed with similar inlet temperature/ flow conditions and a corona current of 30 μA and capillary voltage of 750 V. HgX_2 was detected in SIM mode for m/z of 290−295 ($HgCl_2$) and 378−383 ($HgBr_2$), with the principal signal for the compounds taken as the height of m/z = 291 and 381, respectively.

Sorbent Trap Packing. In addition to polysulfide and shredded Teflon traps, we also tested the performance of magnetite, silver pellet, cobalt chloride, and glass wool traps for collection of HgX_2. Construction of these traps was as described in Sorbent Trap Desorption: Timing and Temper-ature. A full-Teflon trap consisting of shredded Teflon packed into a 6 mm PFA tube was also tested. HgX_2 was collected from air pumped through the $HgCl_2$ particle or mixed mercury halide standard for typically 1 min at 1 L min^{-1}, followed by desorption into the APCI source at 150−200 °C. APCI source parameters were set to the optimums described below in APCI Parameter Optimization, using the SF_6/IB CI blend. HgX_2 was detected in SIM mode for *m*/*z* of 290−295 ($HgCl_2$) and 378− 383 ($HgBr_2$), with the principal signal for the compounds taken as the height of *m*/*z* = 291 and 381, respectively. Results can be found in Table S2, Supporting Information.

HgX_2 Breakthrough and Retention. Initial HgX_2 break- through testing involved two polysulfide traps connected in series with a $HgCl_2$ source, flowing air through the standard onto the traps at 1 L min^{-1} for varying exposure times (5 s−14 min). After exposure, traps were removed and inserted into the APCI inlet for IB/N_2 analysis. The order of traps was noted; the proportion of total HgX_2 collected on each trap gave a measure of trap breakthrough. The order

of traps was changed between runs to prevent possible order bias on the results. A total of 17 runs was collected.

For Teflon traps, we compared the Hg mass collected on a KCl denuder from direct exposure to a mixed HgX_2 standard to the mass of Hg collected with a shredded Teflon trap connected in-line between the denuder and the same HgX_2 standard under identical conditions. Flow through the standard to the denuder was 1 L min^{-1} for 10 s. After sampling, the denuder was placed in-line with the CV/AFS and heated to 500 °C to decompose trapped Hg(II) for CV/AFS analysis. Meanwhile, the Teflon trap, if used, was capped with paraffin film until analysis. After the denuder analysis, the Teflon trap was placed back in-line with the denuder (at room temperature), wrapped in heating tape, connected to a UHP nitrogen source, and heated to 200 °C for 1 min under a N_2 flow of 1 L min^{-1} to transfer collected HgX_2 onto the denuder. The denuder was then reconnected to the CV/AFS for heating and Hg analysis. The elevated concentrations emitted by our standards (μg Hg m^{-3}) preclude testing of long-term retention of Hg(II) on our sorbent traps. To assess HgX_2 retention, we began by collecting HgX_2 onto the Teflon trap as described above. The HgX_2-containing trap was then connected to the UHP N_2 line and left under a flow of 1 L min^{-1} N_2 for 24 h. At the end of 24 h, the trap was connected back in-line with the KCl denuder, wrapped in heating tape, and heated to 200 °C for 1 min under a N_2 flow of 1 L min^{-1} to transfer retained HgX_2 onto the denuder for decomposition to Hg^0 and CV/AFS analysis.

Air Analyses, McGill University, Montreal Quebec, Canada. Air samples were collected during Fall 2013 and Winter 2014 from the roof of Burnside Hall (~60 m height) on the McGill campus for same-day analysis by APCI-MS (SF_6/IB method). Typically, two of the traps were a polysufide and a shred Teflon trap, with a third trap for alternate trap compositions. Air sampling for all traps was 1 day in length (4 PM to 4 PM).

Traps were blanked in the APCI inlet at 200 °C before being plumbed via PFA connectors and tubing to rotometers connected in parallel to a field pump. Trap inlets were exposed directly to the air. Traps were wrapped in heating tape at 50 °C to inhibit water condensation. At the end of sampling, traps were removed from the manifold, sealed with paraffin film, placed in new plastic bags, and transported into the laboratory for analysis. Time between the end of sampling and analysis was typically 15−30 min. Traps were analyzed as described in Sorbent Trap Desorption: Timing and Temperature.

To test whether $HgCl_2$ may be produced by chlorine emitted by swimming pools, we installed the air sampling equipment on the deck of the Memorial Pool at McGill University from January to March 2014. Samples were collected for 12 h overnight (10 PM to 10 AM). Sampling setup and analysis was identical to the setup installed on Burnside Hall.

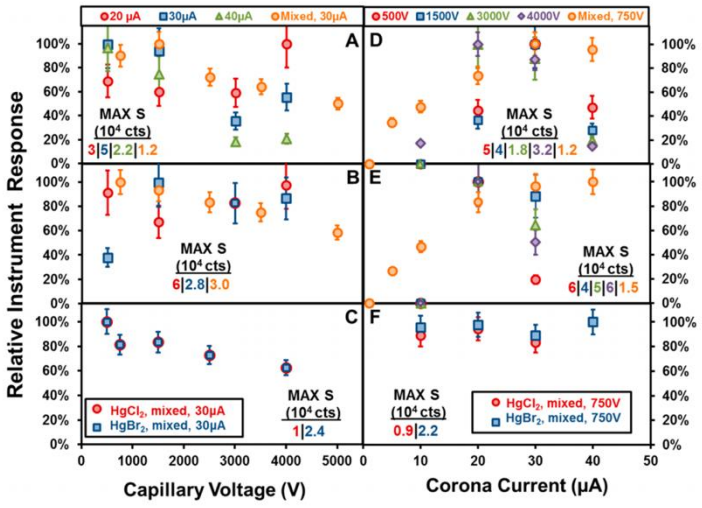

Figure 1. Comparison of the APCI-MS response with varying capillary voltage (left-hand side plots) or corona current (right-hand side plots) for $[HgCl_2 + 26]^-$ (A, D) and $[HgBr_2 + 26]^-$ (B, E) using a 10:90 IB/N_2 CI gas blend and for both compounds (as $[M + 19]^-$) using a SF_6/IB CI blend (C, F). Most tests used single HgX_2 standards with the exception of those marked "mixed" which used the 50:50 $HgCl_2$/$HgBr_2$ mixed standard (described in Source Modification and CI Gas Selection). Values are relative responses (% of maximum signal) segregated by corona current (in μA, for capillary voltage tests) or by capillary voltage (corona current tests) and are the mean of 3−6 measurements, with standard deviations of around ±30%.

https://pubs.acs.org/doi/abs/10.1021/ac504545w

RESULTS AND DISCUSSION

APCI Parameter Optimization. Figure 1 displays HgX_2 ion complex production at varying capillary voltage and corona current for IB/N_2 or SF_6/IB CI gases. Broad patterns are evident, and optimal conditions for APCI analysis of HgX_2 are discussed below.

The response of the APCI-MS to $HgCl_2$ generally decreased with increasing capillary voltage (Figure 1a,c). The $HgBr_2$ signal was relatively constant with increasing capillary voltage for the single standard but decreased for the mixed standard (Figure 1b,c). The discrepancy may arise from comparison of the more variable flux coming off fine powder single-compound standards versus the large-particle mixed HgX_2 standard. The relative decrease in [HgX_2 + 19] with increasing capillary voltage was similar for both $HgBr_2$ and $HgCl_2$ using either CI gas. Capillary voltages in the range of 750−1500 V are optimal for APCI analysis of HgX_2.

In this study, corona current optimization balances CI gas fragmentation with ion complex preservation. The effect of these competing phenomena is illustrated in the peak HgX_2 signal for corona currents of 20−30 μA (Figure 1d−f). When using 10:90 IB/N_2 as a CI gas, lower corona currents (<20 μA) resulted in little to no $[M + 26]^-$ formation, presumably due to limited isobutane fragmentation. At high corona current, the $[M + 26]^-$ yield either decreased or remained constant, suggesting that analyte was lost to fragmentation and/or complexation with an ionized contaminant. For APCI using SF_6/IB, the yield of $[M + 19]^-$ was relatively constant with varying corona current. At a capillary voltage of 750−1500 V, the optimal corona current for APCI analysis of HgX_2 is 30 μA.

The fate of HgX_2 with nonoptimal corona currents varied depending on which HgX_2 standard was used; scans ($200 \leq m/z \leq 500$) of single HgX_2 standards with the IB/N_2 CI blend showed the predominant complex formed at low and high corona current was $[HgX_3]^-$. $HgBr_2$ from the single standard runs was converted into $[HgBr_2Cl]^-$, not $[HgBr_3]^-$, in the ion source, suggesting that chloride contamination was not solely from analyte fragmentation. The sorbent traps used for single $HgBr_2$ tests contained DCDMS-coated glass wool packing; it is probable that at inlet temperatures of 200 °C chlorine- containing gases were emitted from the glass wool into the source. Tests using the mixed HgX_2 standard involved direct introduction of an analyte-rich gas stream without preconcentration. Scans of the mixed HgX_2 standard predominantly showed $[M + 32]^-$ at corona currents <20 μA and [M + 16], [M + 17], and [M + 32]− at a corona current of 40 μA, consistent with complexation with atomic oxygen (O−, m/z = 16), hydroxide (OH−, m/z = 17), and molecular oxygen (O2 −, m/z = 32) formed from molecular oxygen and water in the ion source.

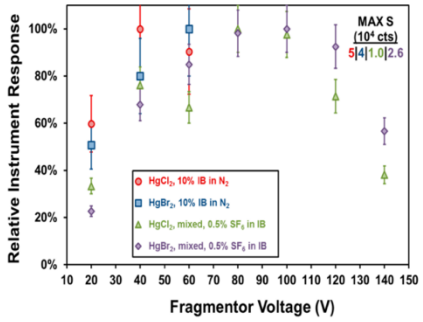

Figure 2. Comparison of the APCI-MS response with varying fragmentor voltage for $HgCl_2$ and $HgBr_2$ using either a IB/N_2 or SF_6/IB CI blend. IB/N_2 tests used single HgX_2 standards while SF_6/IB runs used the 50:50 $HgCl_2$/$HgBr_2$ mixed standard (described in Source Modification and CI Gas Selection). Values are relative responses (% of maximum signal) and are the mean of 3 measurements, with standard deviations of around ±10−30%.

Figure 2 shows the APCI response to HgX2 for varying fragmentor voltage. Initial tests using the IB/N2 CI blend at voltages of 20−60 V suggested that ion transmission was relatively constant for voltages >20 V (Figure 2). Later, tests using SF6/IB at voltages of 20−140 V indicate the highest ion transmission between 80 and 100 V (Figure 2). We therefore selected a fragmentor voltage of 80 V as optimal for HgX_2 measurement.

Figure S12, Supporting Information, plots the APCI response to HgX_2 with varying drying gas temperature and flow rate. In routine APCI-MS, the drying gas evaporates solvent, facilitating charge transfer to the solute, and acts as a screening gas to prevent neutral molecule transmission into the MS. Additionally, the drying gas temperature must be sufficiently elevated to prevent HgX_2 adsorption to the capillary inlet. These conditions were met by increasing drying gas flow rate and temperature to 5 L min^{-1} at 200 °C (Figure S12,

Supporting Information). Increasing the flow rate past 5 L min^{-1} might decrease instrument sensitivity to HgX_2, due to increased N_2 concentrations in-source or to lower HgX_2 residence times in the APCI inlet.

HgX_2 Breakthrough and Retention. For exposure times of ≤7.5 min, $HgCl_2$ was observed only on the first trap in retention tests for polysulfide traps. At exposure times of 10− 14 min, 4−25% of total $HgCl_2$ was collected on the second trap in the series (average of 15 ± 9%, n = 4).

The results of HgX_2 breakthrough and retention tests for Teflon traps can be found in Figure S13, Supporting Information. Average HgX_2 breakthrough through Teflon traps was 28 ± 15% (n = 3). The population mean of HgX_2 collected on a Teflon trap desorbed immediately after loading into the KCl denuder versus after a 24 h pumping of N_2 through the trap at 1 L min^{-1} was not significantly different (n= 3, p = 0.21).

Calibration, Detection Limit Estimation, and Uncertainty. Figure S14, Supporting Information, shows representative calibration curves for APCI analysis of HgX2 standards using either polysulfide preconcentration and the IB/N2 CI gas ("PS:IB") or Teflon preconcentration and the SF6/IB CI gas ("PFA/SF6"). Instrument responses presented in Figure S14, Supporting Information, are the peak height of target masses for HgCl2 and HgBr2. The absolute mass of HgX2 collected on a sorbent trap was estimated from the collection time, and the HgX2 emission rate from the standard (pg HgX2 min−1) was estimated from a concentration of 50 ± 20 ng Hg L−1 and a flow rate of 1 L min−1 . Masses were increased by 28% for Teflon traps and were not adjusted for polysulfide traps, as exposure times were <10 min (HgX_2 Breakthrough and Retention).

Practical equipment constraints prevented trapping of less than 40 ± 10 pg $HgCl_2$ and 50 ± 10 pg $HgBr_2$. To estimate detection limits, we extrapolated from the range covered by calibration curves down to 3σ of the background noise. Detection limits are estimated to be 14 pg $HgCl_2$ and 40 pg $HgBr_2$ for the PS/IB method and 6 pg $HgCl_2$ and 17 pg $HgBr_2$ for the PFA/SF_6 method. Quantities between detection limits and the lowest quantities directly measured are semi- quantitative but mainly cover the range below the limit of quantitation. For a sampling period of 1 day at 1 L min^{-1}, the detection limits presented correspond to concentration-based detection limits of 10 pg $HgCl_2$ m^{-3} and 28 pg $HgBr_2$ m^{-3} by PS/IB and 4 pg $HgCl_2$ m^{-3} and 11 pg $HgBr_2$ m^{-3} by PFA/SF_6.

The sensitivity of the PFA/SF_6 technique was 1.4×10^2 cts pg^{-1} $HgCl_2$ and 5×10^1 counts pg^{-1} $HgBr_2$, higher than sensitivities using PS/IB (6×10^1 cts pg^{-1} $HgCl_2$ and 12 cts pg^{-1} $HgBr_2$). The sensitivity of either technique may be lower than that estimated from single HgX_2 standards due to ion reactions in the APCI source. Concentrations determined using these calibration curves should be considered lower limits to atmospheric HgX_2 concentrations during sampling.

The results presented in Figures 1 and 2 suggest that the reproducibility of HgX_2 preconcentration and APCI analysis is ±30%. Estimates of HgX_2 concentration (pg m^{-3}) include uncertainty from calibration (±40%) and volume sampled (±10%, based on flowmeter variability). Propagating relative errors gives an uncertainty of measurement of ±50%.

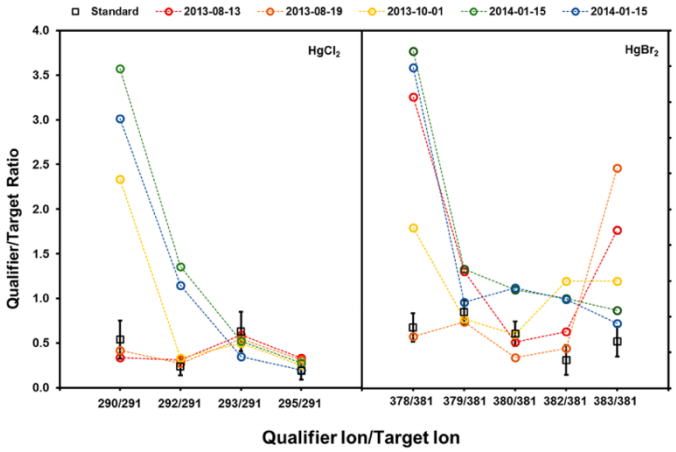

Figure 3. Qualifier/target (Q/T) ion ratios for SIM mode analyses of $HgCl_2$ and $HgBr_2$ in Montreal urban air from August 2013 to January 2014. HgX_2 standard Q/T ratios are shown in black with whiskers equal to 2 times their standard deviation. Sample Q/T ratios falling within the range indicated by whiskers indicate a positive match with standard Q/T ratios.

Air Measurements. APCI analyses of urban and pool air extracts collected on Teflon traps can be found in Figures 3 and S15 and Table S4, Supporting Information. Target ions were m/z = 291 ($HgCl_2$) and m/z = 381 ($HgBr_2$). Qualifier ions for $HgCl_2$ were m/z = 290, 292, 293, and 295 and for $HgBr_2$ were m/z = 378, 379, 380, 382, and 383. Positive identification of HgX_2 was made by comparing sample and standard qualifier− target (Q/T) ion ratios (i.e., the ratio of a qualifier ion signal to the target ion signal). Comparison was considered "excellent" if all sample Q/T ratios were within 2σ of standard Q/T ratios, "good" if 3 Q/T ratios matched, "acceptable" if 2 Q/T ratios were consistent, and "poor" if <2 Q/T ratios matched standard ratios. Representative SIM mode APCI analyses (PFA/SF_6 method) for samples collected at Memorial Pool and Burnside Hall, including trap blanks, are shown in Figure S16, Supporting Information. Trap blanks are significantly smaller than air measurements indicating that compounds detected are not analyte carryover.

$HgCl_2$ detection was excellent in August 2013, good in October 2013, and acceptable in January 2014. $HgBr_2$ detection was acceptable during August and October 2013 and possibly during January 2014, but identification was complicated by highly variable Q/T ratios. $HgCl_2$ detection in pool air was good throughout the sampling campaign, with $HgBr_2$ only detected at an "acceptable" level once during the period. Hg^0 injections through polysulfide and Teflon traps are statistically indistinguishable from direct Hg^0 injections to the CV/AFS (Figure S17, Supporting Information) suggesting that HgX_2 observed does not result from collection of Hg^0 followed by heterogeneous oxidation to Hg(II). HgX_2 concentrations for analytes collected onto shredded Teflon traps ranged from <4 to 1×10^2 pg $HgCl_2$ m^{-3} and <11 to 9×10^1 pg $HgBr_2$ m^{-3} in Montreal urban air and $(4-8) \times 10^1$ pg $HgCl_2$ m^{-3} and <11 to 29 pg $HgBr_2$ m^{-3} in pool air. A fault in the APCI inlet oven lead to incomplete desorption during pool sample analyses, and presented concentrations are lower limits.

CONCLUSIONS AND FUTURE RESEARCH

In this study, we provide the first chemical identification of atmospheric $Hg(II)_{(g)}$ using a novel nano/microparticle extraction-APCI-MS technique. Both $HgCl_2$ and $HgBr_2$ were detected in air extracts. Being trap-based, the technique is portable and shows promise as a valuable tool for studying mercury cycling in the environment. The technique could be extended to other forms of Hg(II) that may be present in the atmosphere, such as HgO or HgI_2. Although in passing, we have shown that aqueous Hg(II) APCI analysis is feasible. Aqueous analysis using a softer ionization technique (electro- spray ionization) may be a valuable avenue of research for a wider range of oxidized mercury in different environmental and nonenvironmental matrices. Optimized APCI-MS analysis of HgX_2 occurs at a

corona current of 30 μA, capillary voltage of 750−1500 V, fragmentor voltage of 80 V, and a drying gas temperature and flow rate of 200 °C and 5 L min^{-1}.

The main weakness of this technique is the frequent presence of coadsorbed contaminants and decreased sensitivity to HgX_2 from unwanted ion reactions in the APCI source. It would be advantageous to develop gas chromatographic separation of collected air samples, although GC separation may be limited by loss of Hg(II) to the column.[11] The current sampling time of 24 h is long and needs to be reduced to bring the temporal resolution of Hg(II) measurements into parity with the much faster GEM and $Hg_{(P)}$ techniques typically used. We foresee that in near future various combination of mass spectrometry techniques (e.g., MS/MS or MS/MS/MS or high resolution units), will further improve identification and quantification of a wider range of mercury species at trace levels.

ASSOCIATED CONTENT

Supporting Information

Additional information as noted in text. This material is available free of charge via the Internet at http://pubs.acs.org.

AUTHOR INFORMATION

Corresponding Author

*E-mail: parisa.ariya@mcgill.ca.

Present Addresses

§F.R.: Department of Chemistry, Shahid Beheshti University, Tehran, Iran.

∥E.-A.G.: Centre for Atmospheric Chemistry, School of Chemistry, University of Wollongong, Wollongong, Australia.

Author Contributions

All authors contributed meaningfully to the preparation of this manuscript. The final version of the manuscript was reviewed and accepted by all of its authors.

Notes

The authors declare no competing financial interest.

ACKNOWLEDGMENTS

We thank H. Khan and Y. Eid for their aid in method development. We also thank P. Carpenter and D. Jacques for allowing us access to the Memorial Pool and Burnside roof for sampling. Funding for this study came from the Natural Science and Engineering Research Funding of Canada, Canadian Foundation for Innovation, Idea-to-Innovation, and Environment Canada. We thank Drs. A. Dastoor and C. Banic for their support. This manuscript benefited significantly from the input of three anonymous reviewers.

REFERENCES

(1) Morel, M. M.; Kraepiel, A. M. L.; Amyot, M. *Annu. Rev. Ecol. Syst.* 1998, DOI: 10.1146/annurev.ecolsys.29.1.543.
(2) Amos, H. M.; Jacob, D. J.; Streets, D. G.; Sunderland, E. M. *Global Biogeochem. Cycles* 2013, DOI: 10.1002/gbc.20040.
(3) Streets, D. G.; Devane, M. K.; Lu, Z.; Bond, T. C.; Sunderland, E. M.; Jacob, D. J. *Environ. Sci. Technol.* 2011, DOI: 10.1021/es202765m.
(4) Schroeder, W. H.; Munthe, J. Atmos. Environ. 1998 , DOI: 10.1016/S1352-2310(97)00293-8.
(5) Lin, C.-J.; Pehkonen, S. O. Atmos. Environ. 1999, DOI: 10.1016/ S1352-2310(98)00387-2.
(6) Lyman, S. N.; Gustin, M. S.; Prestbo, E. M.; Marsik, F. J. Environ. Sci. Technol. 2007, DOI: 10.1021/es062323m.
(7) Steffen, A.; Douglas, T.; Amyot, M.; Ariya, P.; Aspmo, K.; Berg, T.; Bottenheim, J.; Brooks, S.; Cobbett, F.; Dastoor, A.; Dommergue, A.; Ebinghaus, R.; Ferrari, C.; Gardfeldt, K.; Goodsite, M. E.; Lean, D.; Poulain, A. J.; Scherz, C.; Skov, H.; Sommar, J.; Temme, C. Atmos. Chem. Phys. 2008, DOI: 10.5194/acp-8-1445-2008.
(8) Tong, X.; Barat, R. B.; Poulos, A. T. Rev. Sci. Instrum. 1999 , DOI: 10.1063/1.1150049.
(9) Stratton, W. J.; Lindberg, S. E.; Perry, C. J. Environ. Sci. Technol. 2001, DOI: 10.1021/es001260j.
(10) Landis, M. S.; Stevens, R. K.; Schaedlich, F.; Prestbo, E. M. Environ. Sci. Technol. 2002, DOI: 10.1021/es015887t.
(11) Olson, E. S.; Sharma, R. K.; Pavlish, J. H. Anal. Bioanal. Chem. 2002, DOI: 10.1007/s00216-002-1602-6.
(12) Lyman, S. N.; Gustin, M. S.; Prestbo, E. M. Atmos. Environ. 2010, DOI: 10.1016/j.atmosenv.2009.10.008.
(13) Lyman, S. N.; Jaffe, D. A. Nat. Geosci. 2012, DOI: 10.1038/ ngeo1353.
(14) Huang, J.; Miller, M. B.; Weiss-Penzias, P.; Gustin, M. S. Environ. Sci. Technol. 2013, DOI: 10.1021/es4012349.
(15) Gustin, M. S.; Huang, J.; Miller, M. B.; Peterson, C.; Jaffe, D. A.; Ambrose, J.; Finley, B. D.; Lyman, S. N.; Call, K.; Talbot, R.; Feddersen, D.; Mao, H.; Lindberg, S. E. Environ. Sci. Technol. 2013 , DOI: 10.1021/es3039104.
(16) Lyman, S. N.; Jaffe, D. A.; Gustin, M. S. Atmos. Chem. Phys. 2010, DOI: 10.5194/acp-10-8197-2010.

(17) McClure, C. D.; Jaffe, D. A.; Edgerton, E. S. Environ. Sci. Technol. 2014, DOI: 10.1021/es502545k.
(18) Engle, M. A.; Tate, M. T.; Krabbenhoft, D. P.; Schauer, J. J.; Kolker, A.; Shanley, J. B.; Bothner, M. H. J. Geophys. Res. D 2010 , DOI: 10.1029/2010JD014064.
(19) Risch, M. R.; Gay, D. A.; Fowler, K. K.; Keeler, G. J.; Backus, S. M.; Blanchard, P.; Barres, J. A.; Dvonch, K. T. Environ. Pollut. 2012 , DOI: 10.1016/j.envpol.2011.05.030.
(20) Obrist, D.; Tas, E.; Peleg, M.; Matveev, V.; Faïn, X.; Asaf, D.; Luria, M. Nat. Geosci. 2011, DOI: 10.1038/NGEO1018.
(21) Hynes, A. J.; Donohoue, D. L.; Goodsite, M. E.; Hedgecock, L. M. In Mercury Fate and Transport in the Global Atmosphere; Mason, R., Pirrone, N., Eds.; Springer: New York, NY, USA, 2009. DOI: 10.1007/ 978-0-387-93958-2_14.
(22) Ariya, P. A.; Peterson, K.; Snider, G.; Amyot, M. In Mercury Fate and Transport in the Global Atmosphere; Mason, R., Pirrone, N., Eds.; Springer: New York, NY, USA, 2009. DOI: 10.1007/978-0-387-93958- 2_15.
(23) Subir, M.; Ariya, P. A.; Dastoor, A. P. Atmos. Environ. 2011 , DOI: 10.1016/j.atmosenv.2011.04.046.
(24) Harland, P. W.; Thynne, J. C. J. J. Phys. Chem. 1971 , DOI: 10.1021/j100692a005.
(25) Meyer, D. E.; Sikdar, S. K.; Hutson, N. D.; Bhattacharyya, D. Energy Fuels 2007, DOI: 10.1021/ef070120t.
(26) Bombach, G.; Bombach, K.; Klemm, W. Fresenius' J. Anal. Chem. 1994, DOI: 10.1007/BF00326246.